

## Indirect observation of the semiconductor-metal transition in AsF<sub>5</sub>-doped *trans*-polyacetylene

M. Audenaert

*Groupe de Physique des Solides, Université Libre de Bruxelles, boulevard du Triomphe, Code Postal 233, B-1050 Bruxelles, Belgium*

(Received 3 January 1984)

New experimental results on the temperature dependence of the electrical conductivity of AsF<sub>5</sub>-doped *trans*-polyacetylene clearly show a transition from a variable-range-hopping conduction mechanism characteristic of a three-dimensional amorphous semiconductor to a high conducting (metallic) state, as a function of the dopant concentration. The temperature behavior of the electrical conductivity for high doping levels has been well fitted with the use of Sheng's model of fluctuation-induced tunneling conduction. The accuracy of the measurements has been shown to be critical in order to be able to choose between those plausible models which are usually evoked. A general model involving both the intrinsic resistance of the fibrils and the resistance of the junctions between these fibrils is proposed. The relative magnitude of these resistances as a function of dopant concentration can explain the observation of a pure  $T^{-1/4}$  law at low concentrations and the observation of a fluctuation-induced tunneling conduction mechanism at the highest doping levels.

### I. INTRODUCTION

Since there has been much current interest in the conducting organic polymer polyacetylene, many experimental results have been obtained on the magnetic, optical, and electrical properties of this system. It is well known that a semiconductor-to-metal transition occurs when polyacetylene is doped at a concentration higher than 1 mol %.

The electrical-conductivity data and the onset of the metallic behavior for AsF<sub>5</sub>-doped polyacetylene have received different interpretations which we are now going to summarize.

Tomkiewicz *et al.*<sup>1,2</sup> proposed a model of metallic islands separated by undoped polymer regions to explain the  $T^{-1/2}$  dependence of the electrical-conductivity data of AsF<sub>5</sub> lightly doped *cis*-polyacetylene, as well as the linear dependence of the Pauli susceptibility as a function of dopant concentration. These metallic islands would grow in size, while increasing the impurity concentration, finally leading to a percolation transition near 1 mol % of dopant concentration. However, instead of observing a metallic temperature dependence of the electrical conductivity above this critical concentration, they found that even a 16-mol % doped sample still exhibited a  $T^{-1/4}$  law,<sup>2</sup> which is characteristic of a three-dimensional variable-range-hopping (VRH) mechanism, while the temperature dependence of the thermoelectric power was found to be linear for this system.<sup>3-5</sup>

An alternative interpretation of the metallic onset in AsF<sub>5</sub>-doped (CH)<sub>x</sub> is supported by measurements of the magnetic susceptibility of AsF<sub>5</sub>-doped *trans*-polyacetylene performed by Ikehata *et al.*<sup>6</sup> They indeed showed that the metallic transition actually occurs near 5 to 7 mol % impurity concentration. These authors used a special doping technique, known as the "slow-doping" technique, which allows a good uniformity of the dopant concentration into

the polymer structure. The relative sharpness of the transition in the Pauli susceptibility around these impurity concentrations argues against the percolation model. A sharp drop of the thermoelectric power from 840 to 20  $\mu\text{V/K}$  has also been observed by Moses *et al.*<sup>7</sup> near 0.2 mol % of AsF<sub>5</sub> concentration. This suggested the existence of two transitions, one at 0.2 mol % which does not actually correspond to the onset of metallic behavior, and one at 7 mol % corresponding to the semiconductor-metal transition which was already observed at 1 mol % in the previous inhomogeneously doped samples.<sup>8,9</sup>

When we compare the experimental data for AsF<sub>5</sub>-doped polyacetylene with those relating to iodine-doped polyacetylene, we observe many similarities which suggest that these systems are almost equivalent. The temperature-dependent conductivity measurements usually yield a better linear dependence<sup>1,2,10-12</sup> when the logarithm of the electrical conductivity is plotted against  $T^{-1/4}$  or  $T^{-1/2}$ . The  $\ln\sigma$ -versus- $1/T$  plot exhibits a strongly concentration-dependent "activation energy" measured at room temperature, varying from 0.35 eV for undoped polyacetylene to  $\sim 0.005$  eV for AsF<sub>5</sub>-doped samples.<sup>10,13</sup> However, when we examine the experimental data more closely, some differences appear. The slopes obtained for the  $T^{-1/4}$  curves are lower for AsF<sub>5</sub>-doped samples than for iodine-doped samples. A quite different dependence is obtained for the thermoelectric power of iodine-doped polyacetylene as a function of temperature.<sup>5,14</sup> Actually, the absence of linearity of the  $S$ -versus- $T$  plot for the highest doping levels argues against the existence of a metallic state for this system. However, Epstein *et al.*<sup>15</sup> showed that the electrical conductivity of iodine-doped polyacetylene could exhibit a temperature dependence characteristic of a dirty metal. On the other hand, Sheng<sup>16</sup> succeeded in fitting the conductivity data of a 22 mol % iodine-doped sample using a model involving a fluctuation-induced tunneling conduction mecha-

nism between large metallic segments separated by an insulator. These observations, however, only increase the confusion inherent in the microscopic interpretation of the transport data of doped polyacetylene.

This paper presents experimental work on temperature-dependent electrical-conductivity measurements whose purpose was to try to discover whether a transition could be observed in the temperature behavior of the conductivity when the AsF<sub>5</sub> concentration is varied around and above 1 mol%. We think that this study clarifies some of the above-mentioned discrepancies.

In order to characterize our samples as well as possible, we limited our work to the study of doped *trans*-polyacetylene. Indeed, it is well known that the *cis*-rich polymer partly converts into *trans*-polyacetylene upon doping.<sup>17</sup> Our experimental data have been fitted using the plausible conduction models evoked. The accuracy of these fits have been compared one with each other. In Sec. II we present the method we used to analyze our data and to compare the quality of these fits. We also derive the important experimental conditions we needed to determine the agreement or the disagreement between the various plausible models and the set of data. In Sec. III we present the experimental techniques used to achieve our goals. In Sec. IV we give a summary of the experimental results which are discussed in Sec. V. The conclusions are given in Sec. VI.

## II. METHOD OF ANALYSIS OF THE EXPERIMENTAL DATA

Let us consider a physical model for which theoretical results yield a relation between the temperature  $T$  and a physical parameter  $S$  (for instance, the electrical conductivity),

$$S = f(T). \quad (1)$$

Let  $S_i, T_i$  ( $i = 1, \dots, N$ ) be the experimental data. We can estimate the deviation of these data from the theoretical model by calculating the expression

$$e = \left[ \frac{1}{N} \sum_{i=1}^N \left[ \frac{S_i - f(T_i)}{S_i} \right]^2 \right]^{1/2}. \quad (2)$$

Multiplying this quantity by 100 gives the deviation in percent. If the function  $f(T)$  contains adjustable parameters, the values of these parameters can be found with the aid of a computer by searching for the minimum value of  $e$ . The good agreement between experimental data and a particular physical model can be determined if the two following conditions are reached simultaneously.

(a) The value of  $e$  obtained for the suitable model must be almost equal to the experimental root-mean-square error (say,  $e^*$ ), provided this error has been accurately calculated.

(b) Any other plausible model which corresponds to a relation  $S = f'(T)$ , which yields a value  $e'$  calculated according to (2), must yield a value of the ratio  $r = e'/e$  sufficiently large to ensure that the experimental data are well fitted by the previous model (for instance,  $r \geq 5$ ).

The ratio  $r$  gives an estimation of the differentiation one is able to make experimentally between two plausible

models. If  $r \approx 1$ , we cannot conclude that the experimental data are in agreement with one of these models. As we will see, the value of  $r$  depends to some extent upon the models which are tried, the experimental error, the range of temperatures investigated, and also the values of the adjustable parameters entering in the relation  $S = f(T)$ .

Let us look at an example of the experimental differentiation between the relations

$$\sigma = \sigma_0 \exp \left[ - \left( \frac{T_A}{T} \right)^{1/4} \right] \quad (3)$$

and

$$\sigma = \sigma'_0 \exp \left[ - \left( \frac{T'_A}{T} \right)^{1/2} \right]. \quad (4)$$

These expressions can be written as

$$\ln \left[ \frac{\sigma}{\sigma_{RT}} \right] = aT^{-1/4} + b \quad (5)$$

and

$$\ln \left[ \frac{\sigma}{\sigma_{RT}} \right] = a'T^{-1/2} + b', \quad (6)$$

where  $\sigma_{RT}$  is the room-temperature conductivity and  $a = -(T_A)^{1/4}$ ,  $b = \ln(\sigma_0/\sigma_{RT})$ ,  $a' = -(T'_A)^{1/2}$ , and  $b' = \ln(\sigma'_0/\sigma_{RT})$ .

For this particular problem, expression (2) yields

$$e = \left\{ \frac{1}{N} \sum_{i=1}^N \left[ \ln \left[ \frac{\sigma_i}{\sigma_{RT}} \right] - aT_i^{-1/4} - b \right]^2 \right\}^{1/2} \quad (7)$$

for the  $T^{-1/4}$  model, and

$$e = \left\{ \frac{1}{N} \sum_{i=1}^N \left[ \ln \left[ \frac{\sigma_i}{\sigma_{RT}} \right] - a'(T_i^{-1/4})^2 - b' \right]^2 \right\}^{1/2} \quad (8)$$

for the  $T^{-1/2}$  model, provided that  $[S_i - f(T_i)]/S_i \ll 1$ .

The different values of  $\sigma_i$  are the experimental conductivity data. The best fits are obtained for both models by minimizing  $e$  with respect to  $a$  and  $b$ , and  $e'$  with respect to  $a'$  and  $b'$ , or by minimizing  $D = Ne^2$  and  $D' = N(e')^2$  with respect to these parameters. If  $\ln(\sigma_i/\sigma_{RT}) = y_i$  and  $T_i^{-1/4} = x_i$ , we obtain the two usual systems of linear equations given by

$$a \sum_{i=1}^N x_i^2 + b \sum_{i=1}^N x_i = \sum_{i=1}^N x_i y_i, \quad (9)$$

$$a \sum_{i=1}^N x_i + Nb = \sum_{i=1}^N y_i,$$

and

$$a' \sum_{i=1}^N x_i^4 + b' \sum_{i=1}^N x_i^2 = \sum_{i=1}^N x_i^2 y_i, \quad (10)$$

$$a' \sum_{i=1}^N x_i^2 + Nb' = \sum_{i=1}^N y_i.$$

If we assume that the experimental data correspond to

the  $T^{-1/4}$  conduction model, we can calculate the values of  $a'$ ,  $b'$ , and  $e'$  from given values of  $a$ ,  $b$ , and  $e$ , provided that we obtain an estimation of  $\sum_i x_i^2 y_i$  in system (10). We can do this by building a set of  $y_i$ 's such that

$$y_i = ax_i + b + (-1)^i e, \quad i = 1, \dots, N. \quad (11)$$

Such a choice of  $y_i$  changes the equations of system (9) by only a negligible quantity. Figure 1(a) shows the calculated values of  $r$  for  $a = -31$  and  $b = 7.56$  as a function of the lower limit  $\Theta$  of the range of temperatures investigated and for  $N = 100$ . The four curves presented are obtained for  $e = 0.005, 0.01, 0.05,$  and  $0.1$ . Figure 1(b) shows the calculated curves for  $a = -10.56$  and  $b = 2.55$ . The values of  $a$  and  $b$  are typical experimental values obtained for doped  $(\text{CH})_x$ . Since we assumed that the conductivity data correspond to the  $T^{-1/4}$  law, we have  $e = e^*$ , where  $e^*$  is the rms error of these hypothetical data.

The following conclusions can be drawn from these figures. First, the experimental differentiation of a  $T^{-1/2}$  from a  $T^{-1/4}$  law becomes almost impossible when  $\Theta \approx 80$  K and  $e > 1\%$ . Second, it is always advantageous, as we could have guessed, to investigate a wide range of temperatures in order to distinguish between both models. Third, since we expect  $e$  to be lower for lower values of the slope  $a$ , the value of  $r$  obtained for samples which exhibit large values of parameter  $a$  will be almost the same as that obtained for samples which exhibit low values of that parameter, provided that the experimental conditions are identical in both cases.

Another plausible model has been obtained by Sheng for a fluctuation-induced tunneling conduction mechanism between metallic segments separated by an insulator.<sup>16</sup> He derived the following relation for the conductivity:

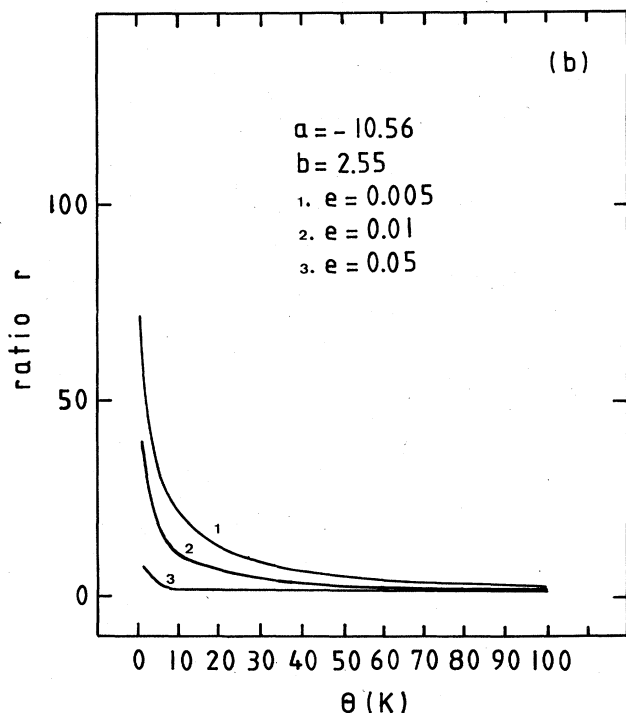
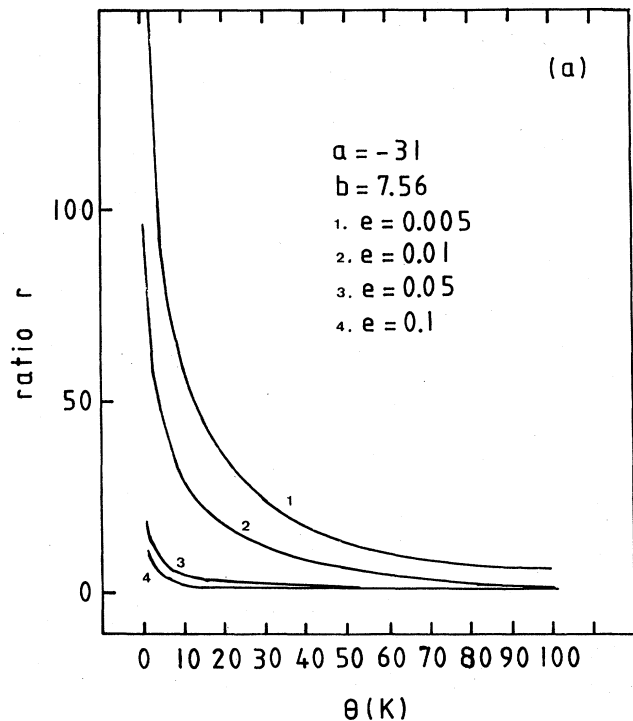


FIG. 1. (a) Ratio  $r = e'/e$  (see text), for differentiation between a  $T^{-1/2}$  and a  $T^{-1/4}$  law, as a function of the lower limit  $\Theta$  of the range of temperatures investigated and for different values of  $e$ ; (b) dependence of  $r$  vs  $\Theta$  for lower values of parameters  $a$  and  $b$ .

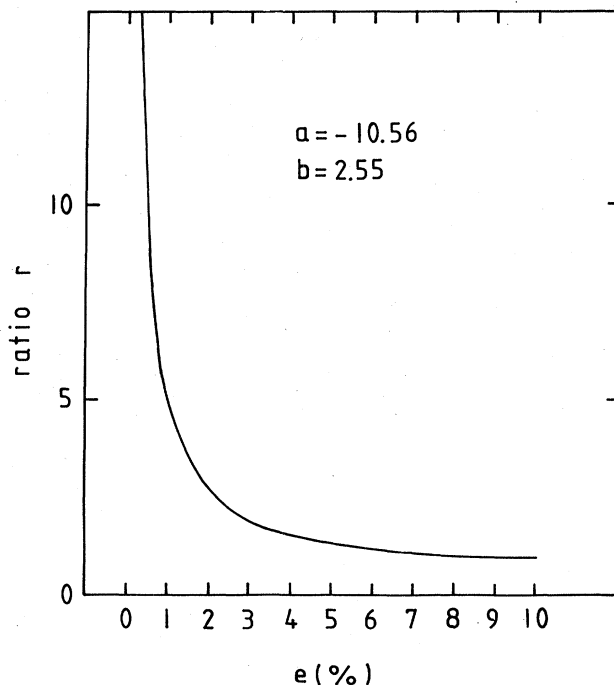


FIG. 2. Ratio  $r = e'/e$  for the differentiation between a  $T^{-1/4}$  law and  $\sigma \sim \exp[-(T_1/T)\epsilon^2 - (T_1/T_0)\varphi(\epsilon)]$  as a function of  $e$ . The range of temperatures investigated lies in the interval  $4.2 < T < 300$  K.

$$\sigma = \sigma_0'' \exp \left[ -\frac{T_1}{T} \epsilon^2 - \frac{T_1}{T_0} \varphi(\epsilon) \right]. \quad (12)$$

We have studied the possibility of experimental differentiation between this conduction model and the VRH model. With given values of  $a$ ,  $b$ , and  $e$ , we obtain the minimum value of  $e'$ , and hence  $r$ , by adjusting the parameters  $T_1$ ,  $T_0$ ,  $\lambda$  (Ref. 18), and  $\sigma_0''$ . Figure 2 shows the calculated values of  $r$  as a function of  $e$  for  $a = -10.56$  and  $b = 2.55$ . The set of hypothetical data corresponding to the  $T^{-1/4}$  temperature dependence are distributed between 300 and 4.2 K with a higher concentration of data at low temperatures. From this figure we conclude that we must keep the experimental rms error below or near 1% in order to be able to choose between (3) and (12).

### III. EXPERIMENTAL TECHNIQUES

Polyacetylene was synthesized following the procedure developed by Shirakawa and co-workers.<sup>19-21</sup> The films, about 150  $\mu\text{m}$  thick, were *trans*-isomerized<sup>22</sup> by heating them at 180°C for 1 h under inert atmosphere, then placed in a storage vessel which was evacuated and held at -196°C. Small pieces of film ( $\sim 1.2 \times 0.5 \text{ cm}^2$ ) were subsequently cut and doped with  $\text{AsF}_5$  at low pressure following the usual "fast-doping" technique. The concentration was measured by weight uptake and checked with a second sample placed near the first during the doping procedure. The dc-conductivity measurements were made using the four-probe method. The electrodes were painted on the surface of the film using Electrodag + 502.

The voltage and current measurements were made using a Keithley-616 electrometer and a Keithley-177 multimeter. To ensure good accuracy, the value of the current was always adjusted to collect the voltage and current measurements with a maximum number of displayed digits and such that the power dissipated in the film was always kept lower than 0.1 mW. The conductivity data were taken after the temperature was allowed to stabilize for a period of 15–20 min. Four voltage-current couples of data (two forward-biased and two reverse-biased) were taken to calculate the conductivity by quadratic linear regression. For each datum the correlation factor of this linear regression was systematically calculated and compared to the preceding one. This allowed us to have continuous control of the quality of measurements within the temperature range investigated. The relative error was as low as 0.22% for current measurements and between 0.25 and 0.60% for voltage measurements. The absolute error of temperature measurements was held below 0.1 K. The values obtained for the experimental rms error  $e^*$  relating to the sets of  $\sim 100$  couples of temperature-conductivity measurements lay between  $5 \times 10^{-3}$  and  $1 \times 10^{-2}$ . The lower values were obtained for samples with low activation energy and the larger values for samples with larger activation energy. Thus, we also expect to find larger values of  $e$  given by (2) for the latter than for the former.

### IV. EXPERIMENTAL RESULTS

*trans*-polyacetylene has been doped at concentrations of  $\text{AsF}_5$  below and above 1 mol %. A typical curve obtained

for an  $\text{AsF}_5$  concentration below 1 mol % is presented in Fig. 3(a), where the logarithm of  $\sigma(T)/\sigma_{\text{RT}}$  is plotted against  $T^{-1/4}$ . These data concern a 0.5-mol % doped sample. The curve of Fig. 3(b) concerns the same sample which was kept at room temperature for 3 d under an inert atmosphere of helium. For these data, the best fit is obtained for  $\sigma \sim \exp[-(T_A/T)^{1/4}]$ .

As we can see, the deviation observed at low temperatures tends to disappear with time. Freshly prepared samples exhibit a significant macroscopic inhomogeneity of dopant distribution along the thickness of the film. This initial inhomogeneity of dopant distribution occurs when the fast-doping technique is used and is probably respon-

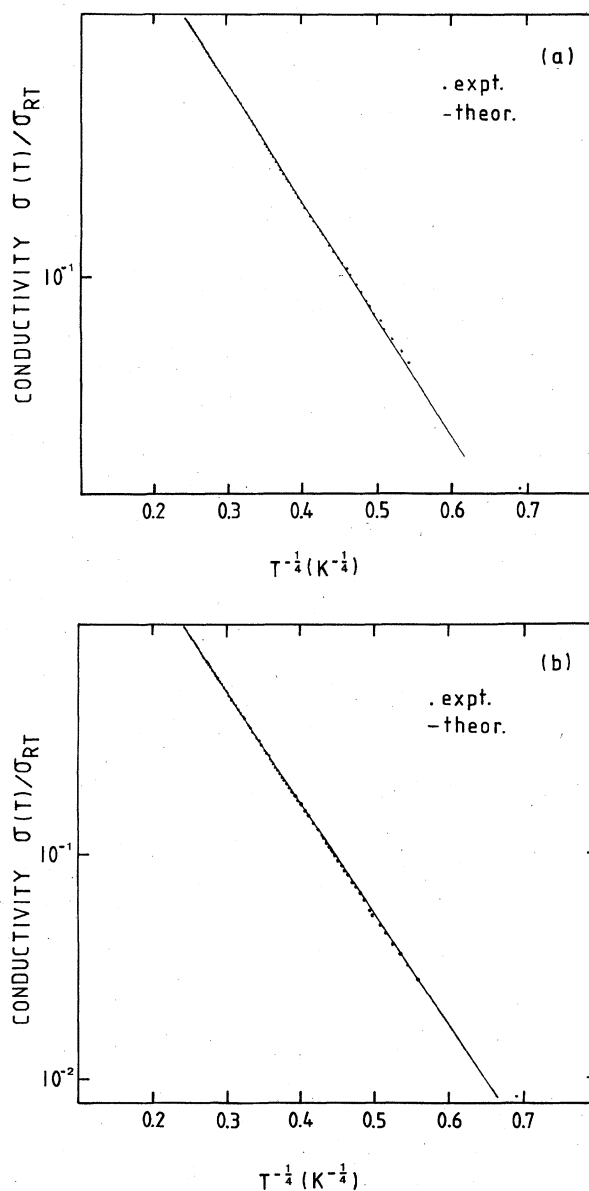


FIG. 3. Logarithm of  $\sigma(T)/\sigma_{\text{RT}}$  versus  $T^{-1/4}$  for (a) a freshly doped  $[\text{CH}(\text{AsF}_5)_{0.005}]_x$  sample, and (b) the same sample kept under an inert atmosphere of helium, for 3 d at room temperature.

TABLE I. Experimental values of the parameters of formulas (13) and (14);  $N$  denotes the number of data,  $e$  is given by expression (2), and  $T_{\text{in}}-T_{\text{fin}}$  gives the range of temperatures investigated.

Figure	$T_A$ (K)	$N$	$\sigma_{\text{RT}}$ ( $\Omega^{-1}\text{cm}^{-1}$ )	$e$	$T_{\text{in}}-T_{\text{fin}}$ (K)
3(a)	$1.4 \times 10^4$	97	0.46		296-4.2
3(b)	$1.9 \times 10^4$	97	0.35	0.0099	294-4.2

sible for this slight deviation from the  $T^{-1/4}$  law at low temperatures. Indeed, the thin layers near the surface of the film which are doped at higher concentrations are more conducting and exhibit a weaker temperature dependence which is seen at low temperatures. This initial inhomogeneity is probably larger for  $\text{AsF}_5$ -doped than for iodine-doped polyacetylene, due to the difference in size of the dopant molecules. Moreover, such parallel conduc-

tivities were never observed for freshly prepared iodine-doped samples.<sup>23</sup>

The values of  $T_A$  and  $e$  for the data of Fig. 3(b) are given in Table I. The value of  $T_A$  obtained for the data of Fig. 3(a) is equal to  $1.4 \times 10^4$  K at high temperatures. The value of  $e$  for this curve is not significant due to the deviation at low temperatures. The range of temperatures investigated here lies in the interval between room tem-

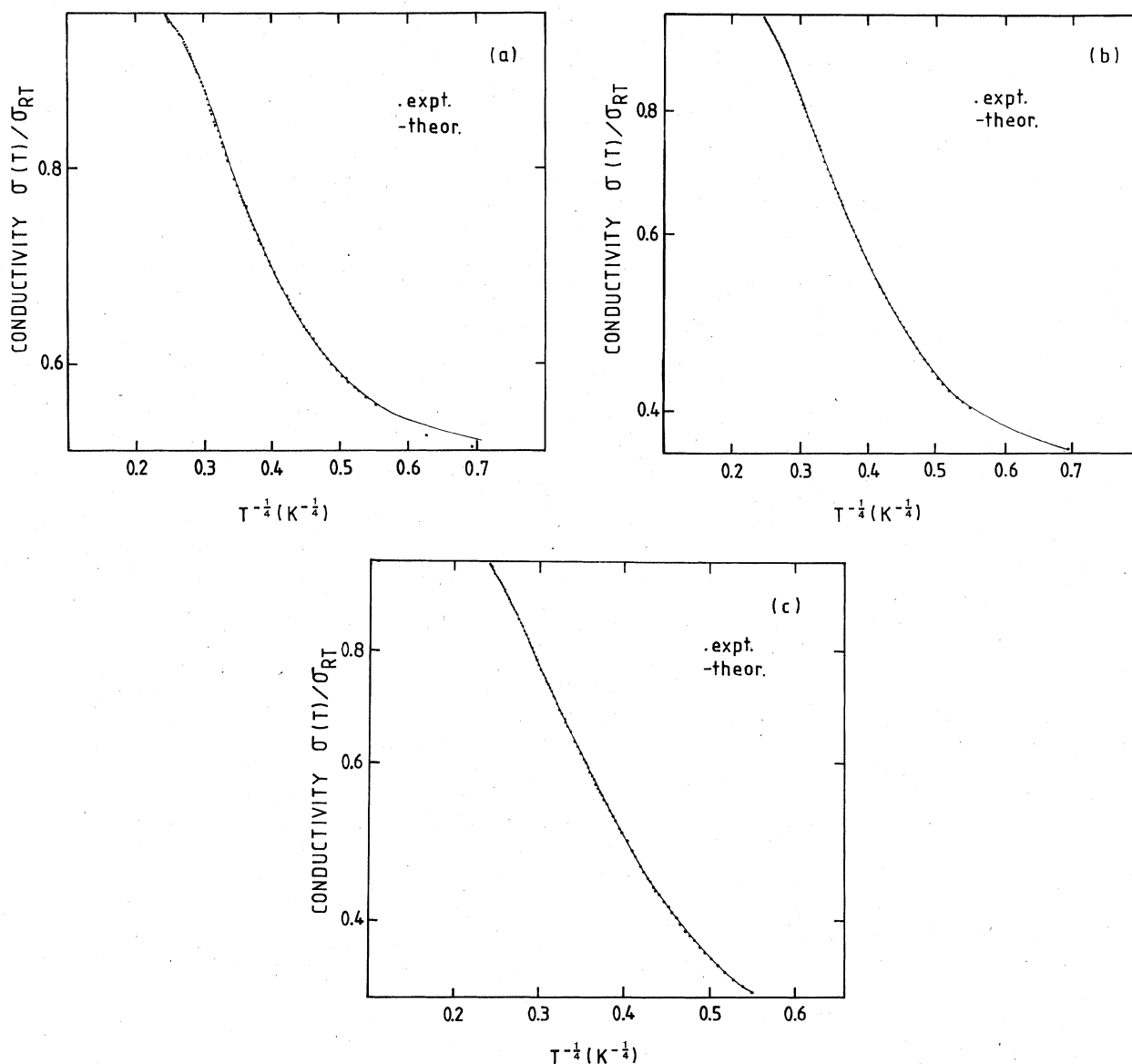


FIG. 4. Logarithm of  $\sigma(T)/\sigma_{\text{RT}}$  versus  $T^{-1/4}$  for (a) a freshly doped  $[\text{CH}(\text{AsF}_5)_{0.11}]_x$  sample, (b) the same sample kept under an inert atmosphere of helium for 4 d at room temperature (RT), and (c) the same sample 7 d after doping.

TABLE II. Experimental values of the parameters of formula (12). The parameter  $\lambda$  governs the shape of the image-force-corrected rectangular potential barrier,  $N$  denotes the number of data,  $e$  is given by expression (2), and  $T_{\text{in}}-T_{\text{fin}}$  gives the range of temperatures investigated.

Figure	$T_1$ (K)	$T_0$ (K)	$\lambda$	$T_1/T_0$	$N$	$\sigma_{\text{RT}}$ ( $\Omega^{-1}\text{cm}^{-1}$ )	$e$	$T_{\text{in}}-T_{\text{fin}}$ (K)
4(a)	24	32.5	0.130	0.74	97	109	0.0048	295-4.2
4(b)	44	36	0.108 75	1.22	95	70.7	0.0037	287-4.2
4(c)	86	54	0.080 00	1.59	96	55.6	0.0039	295-10

perature and 4.2 K. The relative experimental errors  $e^*$  are lower than 1%. The values given in Table I and the analysis made in Sec. II ensure that the experimental conditions enabled us to clearly establish a distinction between a temperature behavior corresponding to expressions (3), (4), or (12).

The conductivity data of a sample, doped at a concentration of 11 mol % are plotted as a function of  $T^{-1/4}$  in Figs. 4(a)-4(c). The absence of linearity of the data is obvious. The range of temperatures investigated is almost the same as above and  $e^* \approx 0.5\%$ . Again, the experimental conditions allowed us to determine the right model. The best fit is obtained for Sheng's model given by expression (12). Figure 4(a) shows the temperature behavior of the electrical conductivity of a freshly prepared sample. Figures 4(b) and 4(c) represent  $\sigma(T)$  for the same sample which was kept for 4 and 7 d, respectively, under an inert atmosphere of helium at room temperature. The values obtained for parameters  $T_1$  and  $T_0$ , and the values of  $e$ , are given in Table II. The ratio  $T_1/T_0$  calculated for the three curves of Fig. 4 is related to the "transparency" of the tunnel barriers in Sheng's model.<sup>16</sup>

The data are well fitted by this model and the values obtained for  $e$  indicate that the fit is even better for the data of Fig. 4(c) than for the data of Fig. 4(a). This slight difference is, again, probably a consequence of the redistribution of the dopant with time along the thickness of the sample, which suppresses unequal parallel conductivities, leading to a worse fit. This is also suggested by the increase of the ratio  $T_1/T_0$  with time, which means that the "transparency" of the tunnel barriers decreases. As a matter of fact, we expect the lowering of the local concentration of  $\text{AsF}_5$  in the portions of the film doped at the highest concentrations (near the surfaces), i.e., those portions which contribute significantly to the conductivity, to induce a decrease in barrier transparency due to the displacement of the Fermi energy  $E_F$  within the conducting segments.

The evolution of parameter  $\lambda$  is also meaningful. Indeed, the value of the electrical field  $\mathcal{E}_0$ , for which the barrier disappears, is related to the value of  $\lambda$ , which con-

trols the size of this barrier. However,  $\mathcal{E}_0$  is also related to  $T_1$ . The charging energy of the capacitor, formed by the conducting segments and the insulator, which corresponds to the energy that a charge carrier needs to cross the barrier, is equal to  $v\mathcal{E}_0/2$  where  $v$  is the volume of the capacitor. This energy is also equal to  $k_B T_1/2$  (derived by Sheng from the application of the equipartition theorem to this system with one degree of freedom). The values of  $T_1$  and  $\mathcal{E}_0^2$ , the latter being the square of a reduced form of the electrical field  $\mathcal{E}_0$ , are given in Table III for the three curves, Figs. 4(a)-4(c). These values were obtained at the three different times,  $t_1$ ,  $t_2$ , and  $t_3$ , such that  $t_1 < t_2 < t_3$ . The ratio  $T_1(t_2)/T_1(t_1)$  is equal to 1.83, i.e., very near the ratio  $\mathcal{E}_0^2(t_2)/\mathcal{E}_0^2(t_1)$ , which is equal to 1.74. Likewise, the ratio  $T_1(t_3)/T_1(t_1)$ , equal to 3.58, is very close to the value of  $\mathcal{E}_0^2(t_3)/\mathcal{E}_0^2(t_1)$ , which is equal to 3.96. This means that the average volume  $v$  of the barriers remains constant with time when the dopant is redistributed and suggests that the barriers are geometrically independent of the dopant.

In Fig. 5 we show the evolution with time of the ratio of the room-temperature conductivity to the initial room-temperature conductivity. When the sample is kept under an inert atmosphere, the electrical conductivity only drops to  $\sim 50\%$  of its initial value in a period of 9 d.

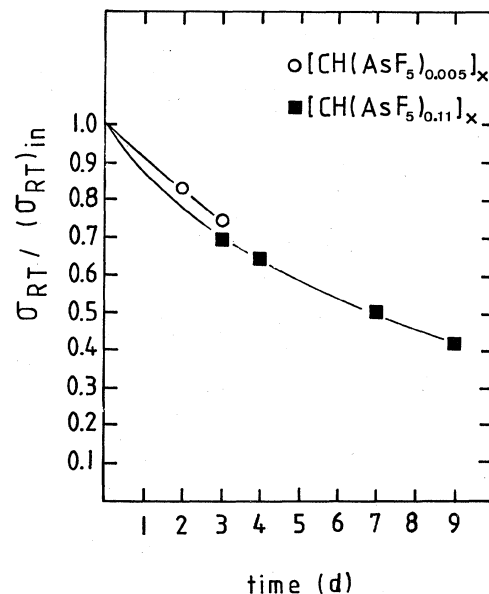


FIG. 5. Evolution with time of the normalized electrical conductivity of  $\text{AsF}_5$ -doped samples at room temperature.

TABLE III. Values of  $\lambda$ ,  $T_1$ , and the square of the reduced electrical field  $\mathcal{E}_0^2$ , for three different times such that  $t_1 < t_2 < t_3$ .

Time	$\lambda$	$\mathcal{E}_0^2$	$T_1$ (K)
$t_1$	0.130 00	1.64	24
$t_2$	0.108 75	2.86	44
$t_3$	0.080 00	6.50	86

## V. DISCUSSION

Our experimental data clearly show that  $\text{AsF}_5$ -doped *trans*-polyacetylene has a temperature dependence of its conductivity which is typical of a three-dimensional variable-range-hopping mechanism when the concentration of dopant is lower than about 1 mol %. The conduction tends to a high conducting (metallic state) at high dopant concentrations, as was expected from the theoretical studies of Mele and Rice.<sup>24</sup> We have been able to indirectly demonstrate this transition of the macroscopic transport properties by testing Sheng's expression of the conductivity for a model involving high conducting segments separated by an insulator. The tunnel barriers are probably made of junctions between the crystalline fibrils and are not induced by an inhomogeneous dopant distribution since the redistribution of the dopant with time did not alter the average volume of these barriers. This suggests that the barriers are already "physically" present in pristine polyacetylene and that the overall resistance of a film is, on the average, made up of a sum of two resistances in series which exhibit a different temperature dependence,

$$R(T) = R_I(T) + R_J(T),$$

where  $R_I(T)$  is the intrinsic resistance due to the fibrils and  $R_J(T)$  is the resistance of the junctions between the fibrils. For high doping levels,  $R_J(T)$  is given by expression (12). Three different situations can occur:

- (i)  $R_I(T) \gg R_J(T)$  for all temperatures between 300 and 4.2 K;
- (ii)  $R_I(T) \approx R_J(T)$  for a certain range of temperatures between 300 and 4.2 K;
- (iii)  $R_I(T) \ll R_J(T)$  for all temperatures between 300 and 4.2 K.

The first situation is illustrated by Figs. 3(a) and 3(b). Here, the intrinsic resistance  $R_I(T) = R_0 \exp[(T_A/T)^{1/4}]$  is larger than the overall junction resistance. This temperature dependence of the resistance is also found for freshly prepared iodine-doped samples. When the  $\text{AsF}_5$  concentration is increased, a transition to a high conducting metallic regime occurs, resulting in a dramatic decrease of the resistance of the fibrils. This yields a situation described by relation (iii) above. As shown in Figs.

4(a)–4(c), only the temperature dependence of  $R_J(T)$  is observed. The second situation has been obtained for aged iodine-doped samples and bromine-doped samples.<sup>25</sup> Our results show that only a single and logical interpretation of the transport data of  $\text{AsF}_5$ -doped *trans*-polyacetylene remains possible when the experimental error is kept very low. We must emphasize the fact that only *trans*-polyacetylene was studied in this work and that the same conclusions cannot be drawn *a priori* for doped *cis*-polyacetylene. In view of these new experimental results, it would be interesting to undertake a similar detailed study on homogeneously doped samples as well as on doped *cis*-polyacetylene films.

## VI. CONCLUSIONS

This systematic study of the electrical conductivity of  $\text{AsF}_5$ -doped polyacetylene has shown that, depending on the values of the "activation energies," the experimental error must be kept lower than a critical value of about 1% in order for us to be able to choose between the models which are generally proposed for this system. By lowering the experimental error below this value, we have demonstrated, in agreement with theoretical calculations,<sup>24</sup> that a transition occurs as a function of dopant concentration from a variable-range-hopping conduction mechanism to a high conducting (metallic) state. At high doping levels, the conductivity data are well fitted by Sheng's model of fluctuation-induced tunneling conduction. Furthermore, a general macroscopic conduction model involving two resistances in series has been proposed. The relative magnitude of the intrinsic resistance of the fibrils compared to the resistance of the junctions between these fibrils explains the observation of a pure  $T^{-1/4}$  law at low dopant concentrations as well as the persistence of an activation energy at high dopant concentrations.

## ACKNOWLEDGMENTS

I acknowledge useful discussions with G. Gusman, R. Deltour, F. Masin, and V. Leo, and I thank G. Gusman for a critical reading of the manuscript.

<sup>1</sup>Y. Tomkiewicz, T. D. Schultz, H. B. Brom, T. C. Clarke, and G. B. Street, Phys. Rev. Lett. 43, 1532 (1979).  
<sup>2</sup>Y. Tomkiewicz, T. D. Schultz, H. B. Brom, A. R. Taranko, T. C. Clarke, and G. B. Street, Phys. Rev. B 24, 4348 (1981).  
<sup>3</sup>J. F. Kwak, W. D. Gill, R. L. Greene, K. Seeger, T. C. Clarke, and G. B. Street, Synth. Metals 1, 213 (1979/80).  
<sup>4</sup>J. F. Kwak, T. C. Clarke, R. L. Greene, and G. B. Street, Solid State Commun. 31, 355 (1979).  
<sup>5</sup>Y. W. Park, A. Denenstein, C. K. Chiang, A. J. Heeger, and A. G. MacDiarmid, Solid State Commun. 29, 747 (1979).  
<sup>6</sup>S. Ikehata, J. Kauper, T. Woerner, A. Pron, M. A. Druy, A. Sivak, A. J. Heeger, and A. G. MacDiarmid, Phys. Rev. Lett. 45, 1123 (1980).  
<sup>7</sup>D. Moses, A. Denenstein, J. Chen, A. J. Heeger, P. McAndrew,

T. Woerner, A. G. MacDiarmid, and Y. W. Park, Phys. Rev. B 25, 7652 (1982).  
<sup>8</sup>C. K. Chiang, C. R. Fincher, Jr., Y. W. Park, A. J. Heeger, H. Shirakawa, E. J. Louis, S. C. Gau, and A. G. MacDiarmid, Phys. Rev. Lett. 39, 1098 (1977).  
<sup>9</sup>B. R. Weinberger, J. Kaufer, A. J. Heeger, A. Pron, and A. G. MacDiarmid, Phys. Rev. B 20, 223 (1979).  
<sup>10</sup>C. K. Chiang, Y. W. Park, A. J. Heeger, H. Shirakawa, E. J. Louis, and A. G. MacDiarmid, J. Chem. Phys. 69, 5098 (1978).  
<sup>11</sup>K. Mortensen, M. L. W. Thewalt, Y. Tomkiewicz, T. C. Clarke, and G. B. Street, Phys. Rev. Lett. 45, 490 (1980).  
<sup>12</sup>E. K. Sichel, M. F. Rubner, and S. K. Tripathy, Phys. Rev. B 26, 6719 (1982).

- <sup>13</sup>Y. W. Park, A. J. Heeger, M. A. Druy, and A. G. MacDiarmid, *J. Chem. Phys.* **73**, 946 (1980).
- <sup>14</sup>A. J. Epstein, H. Rommelmann, R. Bigelow, H. W. Gibson, D. M. Hoffmann, and D. B. Tanner, *Phys. Rev. Lett.* **50**, 1866 (1983).
- <sup>15</sup>A. J. Epstein, H. W. Gibson, P. M. Chaikin, W. G. Clark, and G. Grüner, *Phys. Rev. Lett.* **45**, 1730 (1980).
- <sup>16</sup>P. Sheng, *Phys. Rev. B* **21**, 2180 (1980).
- <sup>17</sup>C. Mathis and B. François, in *Polymères Electroactifs, Font-Romeu*, edited by P. Bernier and B. Payet (Centre National de la Recherche Scientifique, Montpellier, 1982). See also F. Rachdi, P. Bernier, E. Faulques, S. Lefrant, and F. Schué, *J. Phys. (Paris) Colloq.* **44**, C3-97 (1983).
- <sup>18</sup>The parameter  $\lambda$  controls the magnitude of the correction to the rectangular barrier model; following Sheng,  $\varphi(\epsilon) \approx (1-\epsilon)/(1+\alpha\epsilon+\beta\epsilon^2)$ , where
- $$\alpha = 4.2837 \times 10^{-4} (1/\lambda - 4)^2 + 4.8728 \times 10^{-2} (1/\lambda - 4)$$
- and
- $$\beta = \coth[2.6\lambda/(1-4\lambda)] - (1+\alpha).$$
- <sup>19</sup>T. Ito, H. Shirakawa, and S. Ikeda, *J. Polym. Sci., Polym. Chem. Ed.* **12**, 11 (1974).
- <sup>20</sup>H. Shirakawa and S. Ikeda, *Synth. Metals* **1**, 175 (1979/80).
- <sup>21</sup>C. K. Chiang, A. J. Heeger, and A. G. MacDiarmid, *Ber. Bunsenges. Phys. Chem.* **83**, 407 (1979).
- <sup>22</sup>T. Ito, H. Shirakawa, and S. Ikeda, *J. Polym. Sci., Polym. Chem. Ed.* **13**, 1943 (1975).
- <sup>23</sup>M. Audenaert, G. Gusman, and R. Deltour, *Phys. Rev. B* **24**, 7380 (1981).
- <sup>24</sup>E. J. Mele and M. J. Rice, *Phys. Rev. B* **23**, 5397 (1981).
- <sup>25</sup>M. Audenaert (unpublished).